V_P/V_S mapping – robustness and quality improvement

Albert Zhang and Laurence R. Lines

ABSTRACT

The mapping of V_P/V_S variations provides an effective tool for lithology discrimination. The use of traveltimes from pairs of reflectors on vertical and radial component seismic sections provides a robust and effective means of doing this mapping. The maps provide an effective means to distinguish shales from sandstones in heavy oil fields. Another possible mapping method involves the use of impedance estimation by trace inversions and AVO results. These three mapping techniques provide similar but not identical results. In this paper, we summarize some results of V_P/V_S mapping for heavy oil fields in Western Canada.

INTRODUCTION

Multicomponent seismology is a useful tool for enhanced reservoir characterization of heavy-oil fields. As shown by Watson et al. (2002) and Lines et al. (2005), multicomponent data can provide maps of the P-wave to S-wave velocities (V_P/V_S), and these V_P/V_S maps provide important information about lithology and reservoir changes. In this discussion, we show that V_P/V_S mapping, as derived from traveltime measurements on vertical and radial component data, is a robust procedure.

The fact that this type of mapping was very robust became evident to us when we compared different V_P/V_S maps from several investigators. With the same data and slightly different reflection picks from different horizons, we noticed a striking resemblance of maps – with similar mapping of boundaries. These were evident from comparing maps produced by Lines et al. (2005) to those produced by Zhang and Lines (2005). It would appear that the technique is very robust. Later publications by Dumitrescu and Lines (2006) using AVO analysis also produced similar maps.

We explore two aspects of V_P/V_S mapping using traveltimes. Firstly, we explore the spectral differences of PP and PS seismic volumes and design bandpass filters that can significantly improve the quality of V_P/V_S maps. Secondly, we perform an error analysis of this mapping and show that the derivation of V_P/V_S maps from reflection traveltime picks is not overly sensitive to the choice of reflecting horizons above and below the reservoir.

The computation of V_P/V_S maps from 3C/3D seismic data is straight-forward for flat-layered geology where the vertical component contains predominantly PP reflections and the radial component contains predominantly PS reflections. By picking reflection times for horizons above and below a reservoir on both the vertical and radial components, Watson (2004) (among others) has shown that the V_P/V_S ratio can be derived from the following equation (1):

$$\frac{V_P}{V_S} = \frac{2\Delta t_{PS} - \Delta t_{PP}}{\Delta t_{PP}}, \quad (1)$$

where Δt_{PP} is the interval travel time of the interpreted interval from PP sections and Δt_{PS} is the interval travel time from PS sections. Watson et al. (2002), Lines et al. (2005), and Pengelly (2005) describe successful applications of this mapping to the characterization of different heavy-oil fields in Western Canada.

We noted the robustness of V_P/V_S mapping using multicomponent traveltimes in equation (1) through a sequence of mapping experiments for the Plover Lake data set, as discussed by Lines et al. (2005). Several interpreters constructed V_P/V_S maps using prominent reflectors above and below the target formation, the Mississippian oil sands of the Bakken formation. In these studies, geophysicists were asked to produce V_P/V_S maps by interpreting reflections on the same multicomponent data sets. Although the interpreters picked slightly different reflection events above and below the reservoir zone, it was interesting to see that the various maps were similar to our original map, despite the fact that slightly different reflection events were picked. Although consistency is no proof of correctness, the lithology boundaries on the various maps generally agreed with the core information from the 60 wells in the area. This interesting (and encouraging) mapping result caused us to analyze the robustness of this estimation method.

If the PP and PS sections contain zero-phase wavelets positioned at prominent separated reflectors, the traveltime intervals (isochrons) are relatively insensitive to spectral differences between wavelets. This can be seen by examining modeled seismic traces of Figure 1a. We compare traces with the same arrival times which contain Ricker wavelets (polarity reversed) with peak frequencies of 40 Hz and 20 Hz respectively. By picking the peaks of these wavelets, we note that traveltime picking of traces 1-10 (with 40 Hz Ricker wavelet) and traces 11-20 (with 20 Hz Ricker wavelet) both produce reflection events whose arrivals are at 100 ms and 150 ms respectively, giving isochron values of 50 ms on both sets of traces–despite the factor of 2 difference in the peak frequencies of the wavelets. If the significant reflectors in this analysis are separated by more than the tuning thickness, the traveltime method is very robust and not adversely affected by the peak frequencies of the wavelets. As the reflectors become more closely spaced, there will be greater tuning effects. It should be noted that synthetic seismograms obtained from dipole sonics in this field are very useful in identifying the appropriate reflectors on both the vertical and radial component seismograms.

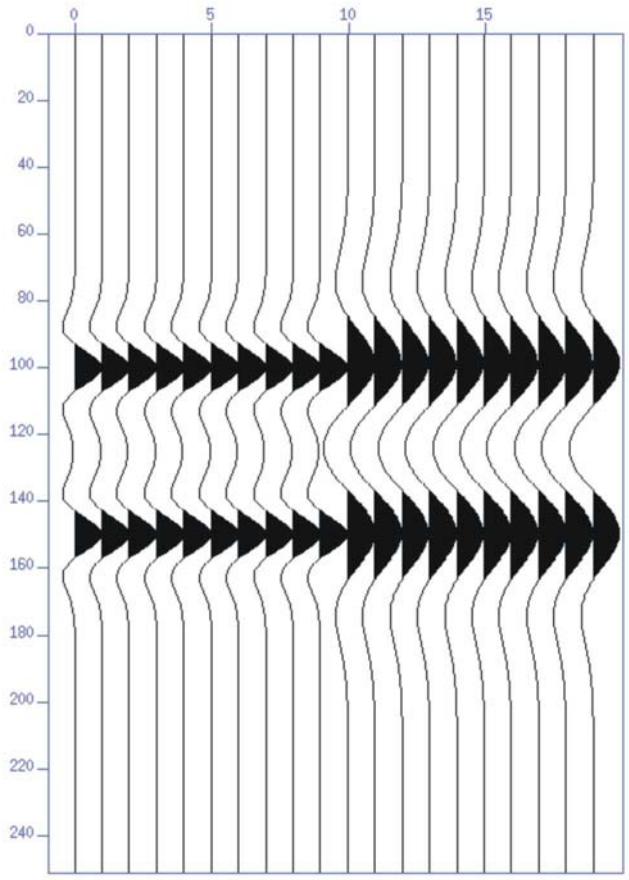

FIG. 1a.. Robustness of traveltime picks for zero-phase wavelets with different spectral content. Traces 1-10 contain Ricker wavelets with peak frequencies of 40 Hz, and traces 11-20 contain Ricker wavelets with peak frequencies of 20 Hz. On both sets of traces, traveltime picks of the peaks produce isochron values of 50 ms, despite the difference in wavelet spectra. (Time scale is in samples, where 1 sample = 1 ms.).

It turns out that this traveltime method of V_P/V_S mapping for this particular area is reasonably robust and is relatively insensitive to the choice of reflectors or differences in the frequency content between the vertical and radial component. If the reflectors are too widely separated, there will be a degradation in vertical resolution of the target area; hence, we generally attempt to find the strongest reflectors that are immediately above and below the target horizon. The frequency robustness is fortunate, since for many multicomponent data sets, there is often a big difference between the frequency spectra of PP and PS seismic volumes. For target reflectors on the two seismic sections, the frequency band of the PP spectrum is usually wider than that of the PS spectrum. With the dominant frequency of PP data usually being higher than for the PS data in this area, it might initially seem that these spectral differences could have a negative effect on the accuracy of calculated V_P/V_S ratios. However, if the wavelets in our data are consistently zero phase and the reflectors are distinctly separated, traveltime picks of peaks and troughs are relatively insensitive to spectral differences between data types.

In practice, it is often difficult to resolve reflections from the top and bottom of the target layer, especially for the PS seismic data. The reflected events from the top and bottom of the pay zone are often incoherent and difficult to pick. In such cases, we will have to select the reference horizons from above and below our target formation. If the interpreted interval between picked top and bottom horizons is thicker than the actual target layer, the calculated V_P/V_S will be smeared or affected by its surrounding layers. In such cases, the error of V_P/V_S from surrounding formations should be analyzed in order to implement the application of V_P/V_S correctly.

Although we note that the picking is relatively insensitive to spectral differences between components, we will show that bandpass filtering can provide some improvement to the quality of V_P/V_S maps. Then, through error analysis, we explain why this mapping procedure is very robust. We also will demonstrate that the V_P/V_S map is not overly sensitive to the choice of picking surrounding formations.

Spectral differences between PP and PS seismic data

As previously mentioned, the frequency spectra of PP and PS seismic volumes in the depth of our target formation are often quite different. Figure 1b shows typical amplitude spectra for wavelets extracted from PP and PS seismic data at Plover Lake. The frequency band of PP spectrum is wider than that of the PS spectrum and the dominant frequency of PP data is usually much higher.

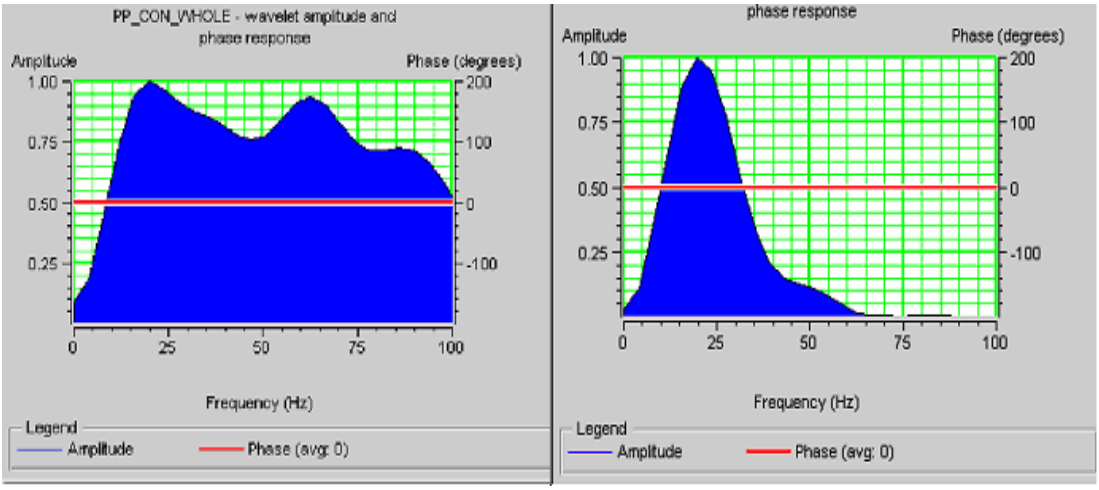

FIG. 1b. Amplitude spectra of wavelets extracted from PP (left) and PS (right) seismic data at Plover Lake field.

To reduce the problem of spectral differences, we applied a low-pass filter to the PP seismic data to the same bandwidth as the PS data. We designed a bandpass filter (0, 10, 30, 55Hz) based on the amplitude spectrum of PS seismic volume, which has a narrower frequency band and a lower dominant frequency, and applied the designed bandpass filter to PP seismic data, which has a wider frequency band and higher dominant frequency. (Another possibility for matching frequencies between the PP and PS data could involve the use of matched filtering instead of bandpass filtering, although the authors have not

yet tested this procedure.) Comparing unfiltered PP data with filtered PP data (Figure 2), we can see the differences of reflection-event character between them. For the top reference horizon, we note that two closely distributed events with higher frequency on the unfiltered PP data merged into one event with lower frequency on filtered PP data. (For easier event correlation, the seismic sections on the left side of Figures 2, 3 and 4 are plotted in reversed direction to those on the right side.) From Figures 3 and 4, we can clearly see that the similarity between PP and PS data is improved after application of band pass filter on PP data, especially for the selected reference top horizon.

The differences on the picked top references between the unfiltered and filtered PP data are shown in Figure 5. The actual difference between picked events (due to the wavelet differences) is not so prominent--being only a few milliseconds, but this will have an effect on the final V_P/V_S maps.

Figures 6 and 7 are the final maps of V_P/V_S between the interpreted reference top and bottom horizons for unfiltered and filtered data. Yellow, orange and red colors show zones of lower V_P/V_S values. Based on our experience with heavy-oil fields in Western Canada, such zones correspond to sand thickening and/or zones affected by heavy-oil production (as described by Watson et al., 2002; Lines et al., 2003; Chen et al., 2003). Generally speaking these maps allow us to detect thickening sand with the initial base survey, whereas we would use time-lapse seismic monitoring to detect reservoir changes.

In Figures 6 and 7, the values of V_P/V_S around production wells are generally lower than elsewhere. The lower values of V_P/V_S have a good correspondence with well locations on both maps, but the map in Figure 7 from filtered PP and PS data has better correspondence with the well data especially in the west-center part. Although our somewhat simplistic initial analysis suggested that the mapping is not overly sensitive to differences in wavelet spectra (Figure 1a), the comparisons of maps in Figures 6 and 7 suggests that it is worthwhile to apply bandpass filtering of the seismic volume to enhance the similarity between PP and PS seismic volumes.

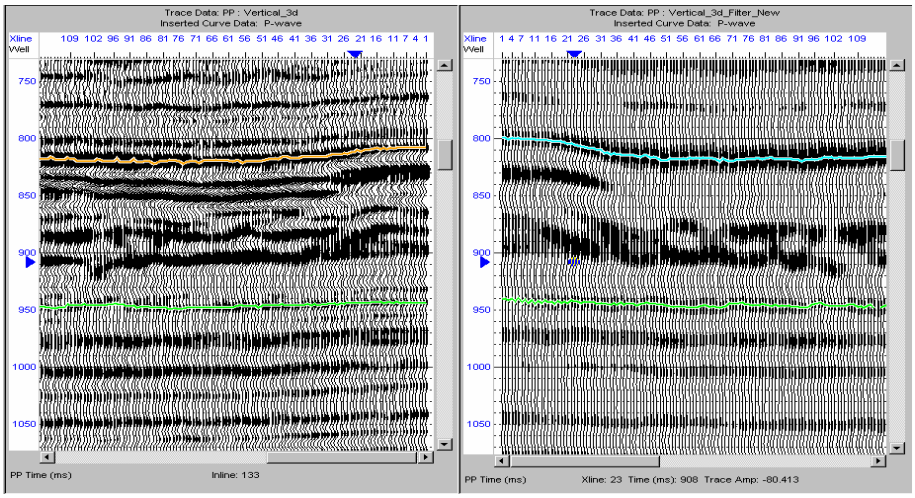

FIG. 2. Comparison between unfiltered PP (left) and filtered PP (right) seismic data (Line on left plots traces 116-1 and line on the right plots traces 1-116).

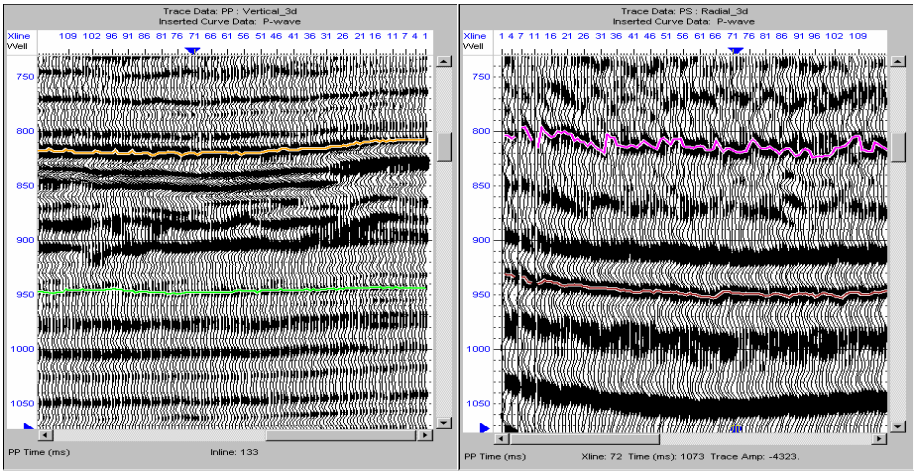

FIG. 3. Comparison between unfiltered PP (left) and PS (right) seismic data. The frequency content of the PP section is much higher than the corresponding PS section.

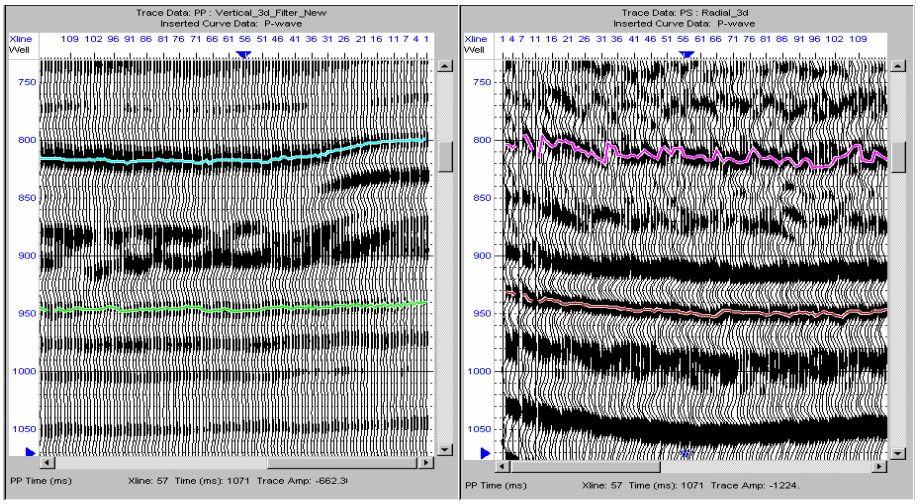

FIG. 4. Comparison between filtered PP (left) and PS (right) seismic data shows a better correlation of reflecting events than in Figure 3.

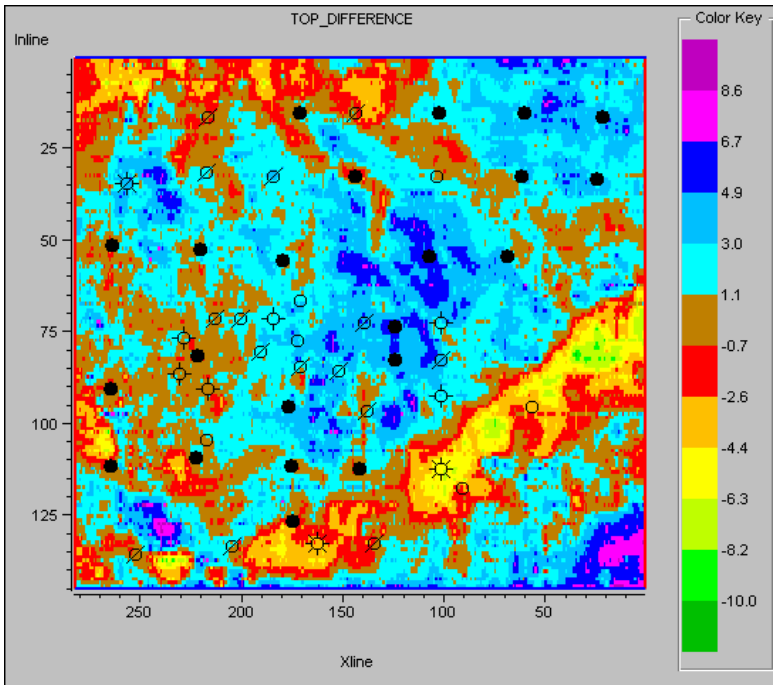

FIG. 5. Difference of top horizons between unfiltered and filtered PP seismic data.

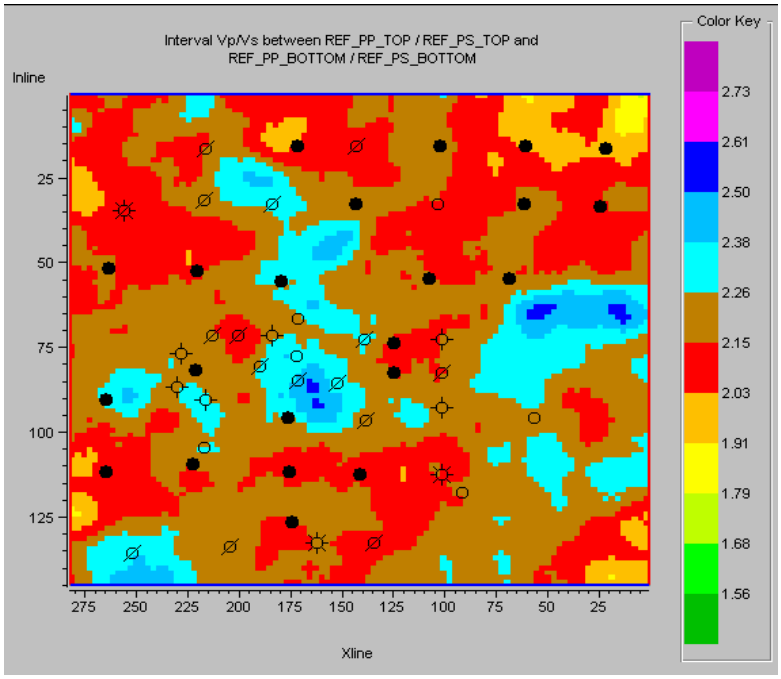

FIG. 6. VP/VS between top and bottom horizons from unfiltered PP and PS data.

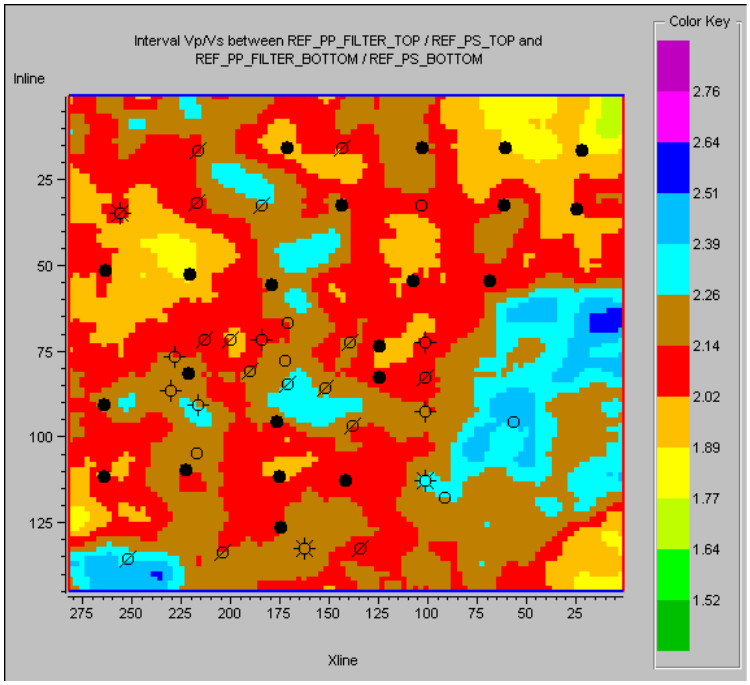

FIG. 7. VP/VS between top and bottom horizons from filtered PP and PS data.

It is interesting that the map in Figure 7 is very similar to the maps obtained by Lines et al. (2005) in which we see slightly different events both above and below the reservoir layer, with the principal difference being that the deeper reference horizon was at about 950 ms in this paper and at 1000 ms in Lines et al. (2005). This similarity of VP/VS maps

suggests that this mapping method is very robust. We now investigate this robustness by error analysis.

Error analysis

In this analysis, we examine the mapping errors introduced by picking reflectors that are slightly above and below the target horizon. The figure is a sketch of the interpreted model of PP and PS data, where V_{P1}, V_P, and V_{P2} are P-wave velocities of surrounding (above-target), target, and surrounding (below-target) formations, V_{S1}, V_S, and V_{S2} are S-wave velocities of surrounding and target formations, Δt_{PP1}, Δt_{PP} and Δt_{PP2} are interpreted traveltimes of surrounding and target formations from PP seismic data, Δt_{PS1}, Δt_{PS} and Δt_{PS2} are interpreted traveltimes of surrounding and target formations from PS seismic data, Δd_1, Δd and Δd_2 are the thickness of surrounding and target formations. We also assume that that the total traveltime interval for PS data is $\Delta T_{PS}=\Delta t_{PS1}+\Delta t_{PS}+\Delta t_{PS2}$, and that the total traveltime for PP data is $\Delta T_{PP}=\Delta t_{PP1}+\Delta t_{PP}+\Delta t_{PP2}$. We set $r_1=V_{P1}/V_{s1}$, $r=V_P/V_S$, $r_2=V_{P2}/V_{S2}$. V_P^* is the average velocity of the P-wave between the interpreted interval and V_S^* is the average velocity of the S-wave between the interpreted interval, then the ratio of V_P^* and V_S^* can be expressed as:

$$R=\frac{V_P^*}{V_S^*}=\frac{2\Delta T_{PS}}{\Delta T_{PP}}-1=\frac{2(\Delta t_{PS1}+\Delta t_{PS}+\Delta t_{PS2})}{\Delta t_{PP1}+\Delta t_{PP}+\Delta t_{PP2}}-1 \qquad (2)$$

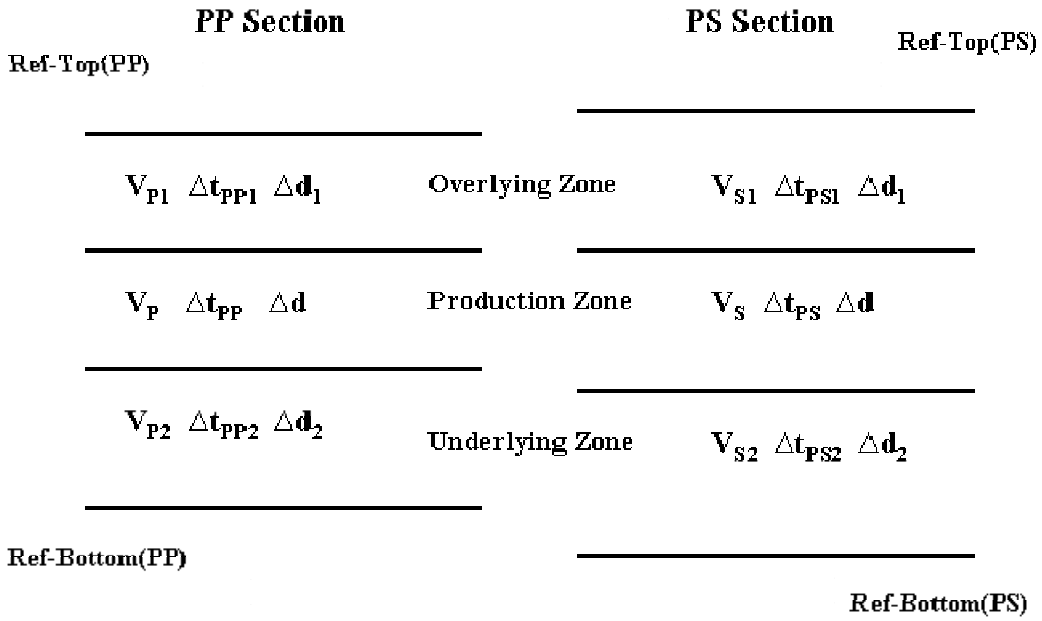

FIG. 8. A sketch of the interpreted model.

The detailed derivation of above and following equations are to be found in Zhang (2005). If $r_1 \approx r_2 \approx 2$ and $V_{P1} \approx V_{P2}$, then:

$$R \approx 2 + \frac{r-2}{\frac{V_P}{V_{P1}} + \frac{V_P}{V_{P2}} + 1} \tag{3}$$

If we set $r_p = V_P / V_{P1}$. the error will be:

$$E = R - r \approx (2-r)\frac{2r_P}{2r_P + 1} \tag{4}$$

The equation of error can be divided into two factors: one is (2-r), another is $2r_p/(2r_p+1)$. The first factor represents the difference in the V_P/V_S ratios between the production zone and surrounding layers (above and below the production zone) since our assumption was that $r_1 \approx r_2 \approx 2.0$. The second factor is the coefficient containing r_p, the ratio of the P-wave velocity in the production zone to the value in the surrounding zone. Since both r and r_p vary laterally, the error will be variable laterally.

In order to examine the error analysis for a simple example, we generate Table 1 of the case where: $V_{P1} \approx V_{P2} \approx 3000$ m/s, and $V_S \approx V_{S1} \approx V_{S2} \approx 1500$ m/s (since velocity of S-wave doesn't change dramatically due to production we set all V_S values to be equal). Based on the above two equations of R and E, the following results are generated for different values of V_P for the target horizon (Table 1).

Table 1. The result of error analysis.

Vp	(Vp1-Vp)/Vp1	Vp/Vs	Vp*/Vs*	E
2000	0.333	1.333	1.714	0.381
2100	0.300	1.400	1.750	0.350
2200	0.267	1.467	1.784	0.317
2300	0.233	1.533	1.816	0.282
2400	0.200	1.600	1.846	0.246
2500	0.167	1.667	1.875	0.208
2600	0.133	1.733	1.902	0.169
2700	0.100	1.800	1.929	0.129
2800	0.067	1.867	1.953	0.087
2900	0.033	1.933	1.977	0.044
3000	0.000	2.000	2.000	0.000

As expected, we note that the estimated values, V_P^*/V_S^*, are close to the actual values V_P/V_S whenever the P-wave velocity of the target zone is close to the value of the surrounding zone. Otherwise stated, the error will increase with the increasing velocity difference between the production zone and surrounding zone. We can also conclude that: if V_{P1}/V_{S1} and V_{P2}/V_{S2} don't change laterally, R will have a similar pattern to that of the ratio r of the production zone. However, if V_{P1}/V_{S1} and V_{P2}/V_{S2} change dramatically laterally, then R will probably reach a different pattern compared with r. Thus, if possible, we should interpret the strongest reference horizons as close as possible to the top and bottom of the production zone to keep the effects of the surrounding zones to a minimum.

In most cases, the production formation is overlain and underlain by formations with the lithology of shale, which act as seal or resource, or both. Shale is usually deposited in a deep water environment and the seismic velocity in shale layers shows little lateral variation. Figure 9 is the impedance inversion result from the PP seismic volume, which shows that overlying and underlying formations are relatively uniform (laterally continuous) compared with the target formation. Moreover, the reflection events from a shaly formation are usually coherent, meaning that they are good candidates for reference horizons. Both of the above facts provide a good condition for us to get a calculated V_P^*/V_S^* map from interpreted intervals, which will have a similar pattern with the V_P/V_S map of target formation.

On the other hand, if the velocities of overlying and underlying formations have a lateral dramatic change due to faulting or a changing depositional environment, we need to analyze the pattern of calculated V_P^*/V_S^* in a restricted area, where the velocities of surrounding formations are relatively stable, so as to improve the reliability of this method.

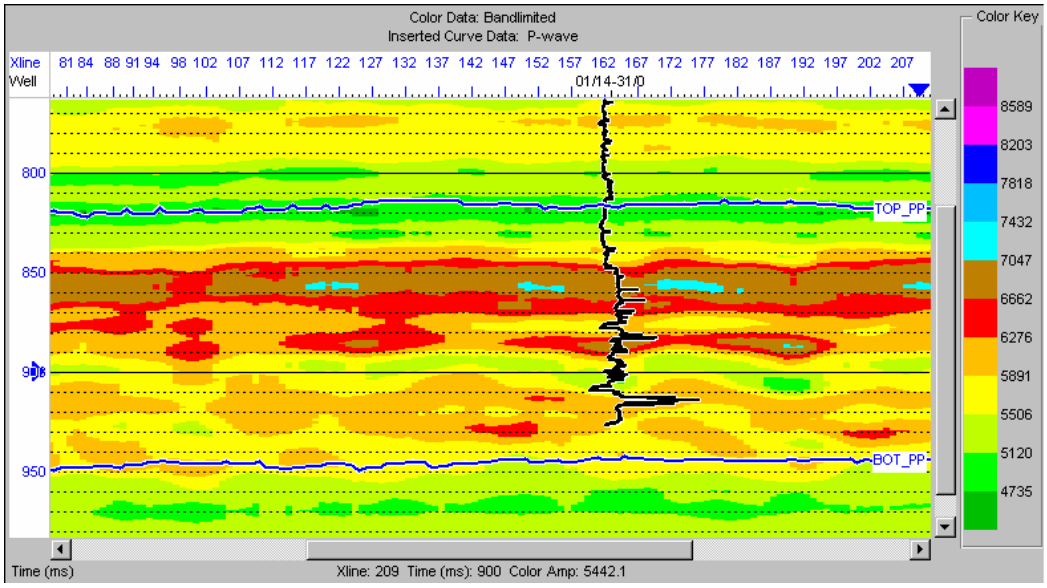

FIG. 9. The impedance inversion result from the PP seismic volume.

CONCLUSIONS

From above analysis and our mapping results, we conclude that the traveltime method for estimating the P-wave to S-wave velocity ratio is not overly sensitive to our choice of reference horizons. Nevertheless, we also conclude that post-stack low-pass filtering of the PP seismic volume will enhance the similarity between PP and PS seismic volumes and will generally help us get a better result. If the velocities of the overlying and underlying formations do not change much laterally, the calculated V_P^*/V_S^* from the interpreted interval will have a similar pattern with the V_P/V_S map of the target formation. Otherwise stated, if the largest lateral change in V_P/V_S occurs at the target horizon, then the lateral change will be shown (albeit in a possibly filtered fashion) in a V_P/V_S estimate obtained over a larger vertical interval. Both our mapping experience and the error analysis demonstrate that traveltime V_P/V_S mapping is very robust for heavy-oil fields such as Plover Lake.

ACKNOWLEDGEMENTS

We would like to thank Joan Embleton, Kevin Hall, Rolf Maier, Richard Xu and Bruce Palmiere for their support and technical discussions. We thank Steve Hill for his constructive editing of this manuscript. We are also grateful to the sponsors of the CREWES and CHORUS projects.

REFERENCES

Chen, S., Lines, L., Embleton, J., Daley, P.F. and Mayo, L., 2003, Seismic detection of cold production footprints of heavy oil in Lloydminster field, CSEG convention, June, Calgary, Alberta, Canada.

Dumitrescu, C.C. and Lines, L., 2006, Heavy oil reservoir characterization using VP/VS Ratios and spectral decomposition, SEG annual meeting, New Orleans, La.

Lines, L., Chen, S., Daley, P.F., Embleton, J. and Mayo, L., 2003, Seismic pursuit of wormholes, The Leading Edge, **22**, 459-461.

Lines, L. R., Zou, Y., Zhang, D. A., Hall, K., Embleton, J., Palmiere, B., Reine, C., Bessette, P., Cary, P., and Secord, D., 2005, Vp/Vs characterization of a heavy-oil reservoir, The Leading Edge, **24**.

Pengelly, K., 2005, Processing and interpretation of multicomponent seismic data from the Jackfish Heavy Oil Field, Alberta, M.Sc. thesis, University of Calgary.

Watson, I. A., Lines, L. R., and Brittle, K. F., 2002, Heavy-oil reservoir characterization using elastic wave properties, The Leading Edge, **21**, 736-739.

Watson, I.A. 2004, Integrated geological and geophysical analysis of a heavy-oil reservoir at Pikes Peak, Saskatchewan, M.Sc. thesis, University of Calgary.

Zhang, D.A. and Lines, L.R., 2005, Vp/Vs and AVO analysis used in monitoring heavy-oil cold production, CREWES Research Report, **17**.